We are IntechOpen, the world's leading publisher of Open Access books Built by scientists, for scientists

4,800
Open access books available

122,000
International authors and editors

135M
Downloads

Our authors are among the

154
Countries delivered to

TOP 1%
most cited scientists

12.2%
Contributors from top 500 universities

CLARIVATE ANALYTICS BOOK CITATION INDEX INDEXED

WEB OF SCIENCE™

Selection of our books indexed in the Book Citation Index in Web of Science™ Core Collection (BKCI)

Interested in publishing with us?
Contact book.department@intechopen.com

Numbers displayed above are based on latest data collected.
For more information visit www.intechopen.com

20

ZrO_2-Bioglass Dental Ceramics: Processing, Structural and Mechanics Characterization

Luiz A. Bicalho[1], Carlos A. R. P. Baptista[2], Miguel J. R. Barboza[2], Claudinei dos Santos[3] and Renato C. Souza[4]
[1]*Universidade Federal Fluminense*
[2]*Universidade de São Paulo*
[3]*Centro Universitário de Volta Redonda*
[4]*Instituto Federal de Educação Ciência e Tecnologia*
Brazil

1. Introduction

The continuous evolution in the development and use of ceramics in various applications, which have hitherto not been considered, have been studied in order to reduce costs and increase the mechanical properties, promoting a longer life applications, with quality assurance.

When considering the use of ceramics in structural materials as materials for implants and implant components, it can be noted as acceptable to meet the demands from the work of mastication, bending fracture strength of about 250MPa and toughness fracture, fracture toughness, about 3MPa.$m^{1/2}$. It is understood that results of these characterizations above indicators guarantees of reliability (ANUSAVICE, 2005).

The polycrystalline tetragonal zirconia is widely used as an agent for other toughened ceramics, because this material has a phase transformation induced by stress, a change of metastable tetragonal phase to monoclinic phase is accompanied by a volume expansion (3-6%), as specialized bibliographies. The transformation absorbs part of the energy required for crack propagation, with an increase in fracture toughness.

Bioglasses are bioactive materials, which are based on the following hypothesis: "The biocompatibility of an implant material is great if the material provides the formation of normal tissue on its surface and, additionally, if it establishes a seamless interface capable of withstanding the loads that normally occur at the site of implantation"(KOHN; DUCHEYNE; AWERBUCH, 1992).

The use of Bioglasses as sintering additives was studied by Amaral (AMARAL, 2002) in Si_3N_4 and Huang (HUANG, 2003) in ZrO_2. This practice reduced the final sintering temperature, without significantly affecting the properties of these materials for dental applications.

In the present work was used as sintering additive, a Bioglass system CaO-P_2O_5-SiO_2-MgO, for application as biomaterial. The use of this additive reduced the final sintering temperature, reducing the manufacturing cost of the product while maintaining the biocompatibility of the product. The bioactive, by having the thermal expansion coefficient

close to the materials used in coatings in cosmetic dental implants, improve the adhesion between implant components based on ZrO_2 and the crown (prosthetic) teeth. It is expected that the Bioglass intergranular additive occupies the interstices and gaps of zirconia and thereby minimize the internal porosity, increasing the mechanical strength and fracture toughness in sintered materials at low temperatures, since the interstices and voids represent the possibility of appearance of micro cracks.
The main objective of this study is to evaluate the microstructural aspects and the physical and mechanical properties of Y-TZP ceramics, $ZrO_2(Y_2O_3)$, sintered, and Bioglass system $3CaO\text{-}P_2O_5\text{-}SiO_2\text{-}MgO$ as an additive to liquid phase sintering.

2. Materials

The materials used in this work were commercially available:
Tetragonal yttria stabilized Zirconia (ZrO2) ceramic Y-TZP containing 3mol% Y2O3, with particle average size of 0.97 μm;Ca $(H_2PO_4)_2.H_2O$, high purity (99.99%); $CaCO_3$, high purity (99.99%); SiO_2, high purity (99.99%) and MgO, high purity (99.99%).

3. Experimental procedures

The necessary procedures of processing steps and characterization of materials used in this work are shown in Figure 1.

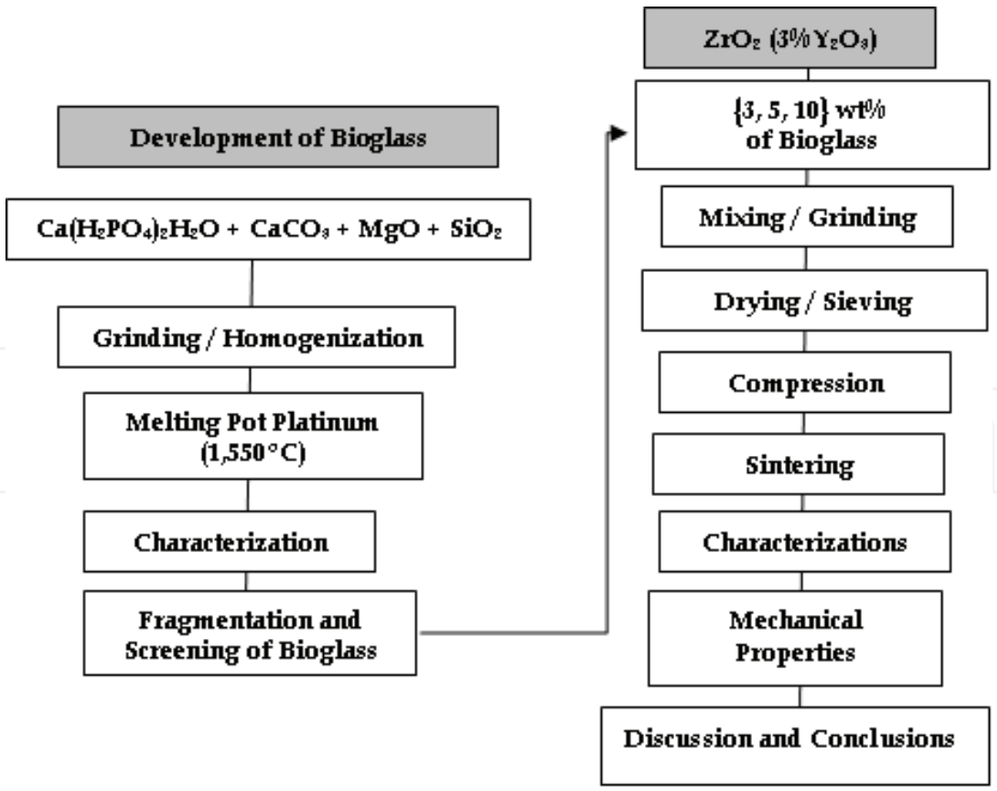

Fig. 1. Flowchart of activities

Was evaluated the content of Bioglass on the results of densification, flexural strength and fatigue, shrinkage during sintering, and the effects on the microstructural configuration. To determine density variations were measured and weighed the compressed green and after sintering.

3.1 Preparation of Bioglass

It was prepared a composition of Bioglass, based on 52.75wt% $CaOP_2O_5$, 30wt%SiO_2, 17.25wt% MgO. This composition was studied by Oliveira (OLIVEIRA et al., 1997) and presented biocompatibility with high bioactivity.

The powders were mixed in a rotary mill for 2 hours using pot stirring rod and polypropylene, in the midst of isopropyl alcohol with zirconia balls for sintered necessary homogenization.

Once mixed, the powders were dried in an oven (110ºC) for 24 hours, sieved (sieve 63µm) and melted at a temperature of 1550°C, the air in a platinum crucible for 2 hours with a heating rate of 10°C/min. The cast (Bioglass) was then rapidly quenched in water at room temperature to obtain better fragmentation and amorphization.

The Bioglass was taken to the oven for drying, and subsequently fragmented with the use of an agate mortar, ground and passed through a sieve of 32µm. The powder, after screening, was subjected to characterization using the techniques of X-Ray Diffraction, Scanning Electron Microscopy (SEM) and Dilatometry.

3.2 Preparation of mixture of powders

Compositions were prepared from powder mixtures, adding distinct Bioglass content ranging from 3 to 5 and 10wt% by weight in the mixture with ZrO_2 (Y_2O_3). Higher values were inviable, since their low mechanical properties due to the small degree of densification, as the evaluations carried out previously by Habibe (HABIBE, 2007).

The raw materials were mixed in attrition mill amid isopropyl alcohol and stirred at 1000 rpm for 2 hours. For every 100g of powder mixtures during milling were used 180g of zirconia balls of sintered with an average diameter of 2mm. The stirring rod and grinding chamber, used herein, are made of polypropylene, to prevent contamination of powder mixtures for possible chafing with the surfaces in contact.

After milling, drying was performed for each mixture, using the vacuum absorption of excess fluid. The drying process was completed in an oven at a temperature of 100ºC for 24 hours. The powders were then subjected to screens: 425, 125, 63 and 32µm. Again it was used agate mortar for each overflow of sieves.

3.3 Sample preparation

3.1.1 Characterization of powders

(i) Thermal analysis of ZrO_2-Bioglass

The coefficients of thermal expansion and glass transition temperature of the compositions were determined by dilatometry using dilatometer - BAHR Thermoanalyse GmbH DIL801L 2000 Model, furnace 7040 (1600ºC). Samples of 3mm x 3mm, 10mm in length were prepared with standard measure based on Al_2O_3, and heated air, heating rate 25°C/min and cooling at 5ºC/min.

(ii) Analysis of phases in mixing of powders

The phases present, both the powders of departure and the powder mixture were identified by X-Ray Diffraction, using diffractometer model XRD-6000 Shimadzu, which is a radiation 'Cu-Kα', with scanning between 20º and 80º, applying step angle of 0.05° and 3 seconds to scan for point counting. The peaks were identified by comparison with JCPDS standard file (JCPDS, 1988).

(iii) Morphology of powders

The powders were observed, the morphology of the particles by analysis by scanning electron microscopy - SEM, LEO 1450VP microscope using EDS and WDS engaged. In the analysis, the powders were coated with thin film of gold and observed using backscattered electron beam, allowing verification by the difference in tone, the phases and morphology of the particles. Were checked by X-Ray Diffraction, the results of possible chemical or crystallographic changes during the stages of milling and compacting the powder mixture.
The study focuses on the compatibility analysis (green density) and concentration of monoclinic phase in the samples to be subjected to sintering.

3.1.2 Characterization sintered

Prior to tests of flexion characterizations were performed for density, hardness, fracture toughness, microstructure and surface phases.

(i) Determination of density

Density of the green bodies was determined by geometric method. The samples were measured in caliper with an accuracy of 0.01mm, and subsequently weighed on analytical balance (10^{-5}g). To a greater degree of accuracy, there were 15 measurements of each sample to obtain an average value reliably.

(ii) X-ray diffraction

The phases present in sintered samples were identified by X-Ray Diffraction using radiation "Cu-K α", scan from 10º to 80º, the step angle of 0.05° and speed of 3 sec/point count. The peaks were identified by comparison with JCPDS file.
Quantification of volume fraction of monoclinic phase (F_M) was calculated from the integrated intensities of monoclinic peaks $(\bar{1}11)_M$ e $(111)_M$ and also the tetragonal peak $(101)_T$.

$$F_M = \frac{1.311X_M}{1+0.311X_M} \tag{1}$$

For which:

$$X_M = \frac{(\bar{1}11)_M + (111)_M}{(\bar{1}11)_M + (111)_M + (101)_T} \tag{2}$$

where: $(\bar{1}11)_M$ 2θ=28.0º; $(111)_M$ 2θ=31.2º; $(101)_M$ 2θ=30.0º to represent the integrated intensity of diffracted peaks plans monoclinic $(\bar{1}11)_M$ and $(111)_M$ in the tetragonal $(101)_T$.

The calculation of the penetration depth of X-rays on the surface was analyzed based on the absorption of these rays by the material. The penetration depth of X-rays was given by equation (3) (KLUG, ALEXANDER, 1974):

$$h = -\frac{sen\theta}{2\left(\frac{\mu}{\rho}\right)\rho}\left[\ln\frac{I}{I_0}\right] \tag{3}$$

with

$$\left(\frac{\mu}{\rho}\right) = w_1\left(\frac{\mu}{\rho}\right)_1 + w_2\left(\frac{\mu}{\rho}\right)_2 + \ldots \tag{4}$$

where:
h = penetration depth [μm];
θ = diffraction angle,
I = intensity of X-ray beam diffracted
I_0 = intensity of X-ray beam focused,
μ = absorption coefficient;
w = weight fraction of component or element;
ρ = density [g/cm³] (Zr = 6.511; O = 1.354; Y = 4.472; $ZrO_2.3\%Y_2O_3$ = 6.051).

(iii) Microstructural analysis

We performed observations of the sintered samples by scanning electron microscopy LEO 1450VP coupled with WDS. To observe the microstructure, the samples were ground and polished according to the procedure mentioned below. After mounting the samples in bakelite, thinning was performed in automatic grinding with diamond paste of particle size, in mesh, from 180 to 600, for the total removal of the inlay material and obtain a flat surface for analysis.

Then the samples were polished with diamond pastes, the sequence of 15, 9, 6, 3 and 1μm. To reveal the grain boundaries, surfaces polished attack suffered heat to air at 1,400ºC for 15 min using a heating rate of 30°C/min to minimize the effects of temperature on grain size. The distribution of grain sizes were measured in order to study the influence of Bioglass on the content of final grain size of ZrO_2 with the purpose of these results are also correlated with the results of mechanical properties. The distribution of grain sizes were measured using image analyzer microscope, LEICA, aimed at studying the influence of Bioglass on the content of final grain size of ZrO_2. These results were also correlated with the results of mechanical properties.

4. Mechanical properties

4.1 Hardness Vickers (HV)

The methodology used to determine the hardness of the samples followed the ASTM C 1327-99, which provides the standard test method to obtain the Vickers hardness of advanced ceramics.

4.2 Fracture toughness (K_{IC})

The methodology for determining the values of fracture toughness by Vickers indentation of the samples followed the recommendations of ASTM C 1421-99. This is the pattern for obtaining the fracture toughness of advanced ceramics at room temperature.

4.3 Flexural strength - 4 points

For the analysis of flexural-bodies were used for proof-polished, dimensions (in mm) 45 x 4 x 3, as previously described. The flexural strength at room temperature, (σ_f) was evaluated by the collapse load of the body of evidence points determined by the method '4 points', following the specifications dictated by the standard DIN EN 843-1 (ASTM C 1161-90) with download speed of 0.5mm/min and with a spacing of 40mm and 20mm between the rollers of support and loading, (I_1 and I_2, respectively) as shown in Figure 2, using a universal machine mechanical testing kN MTS-250.

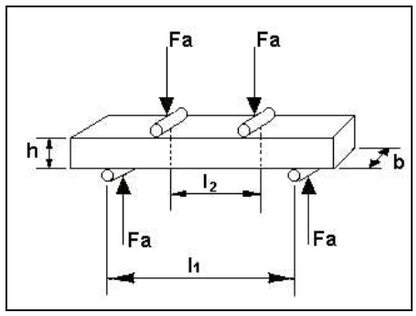

Fig. 2. Schematic representation of resistance to bending in four points. The polished face is turned down (KELLY, 2000).

The flexural strength of the specimens was calculated using Equation 5.

$$\sigma_f = \frac{3}{2} F_A \times \frac{(I_1 - I_2)}{b \times h^2} \quad (5)$$

where:
σ_f = resistance to bending (MPa);
F_A = breaking load (N);
b = measure the width of the samples (mm);
h = height measurement of samples (mm);
I_1 = wider spacing between the rollers loading (mm);
I_2 = smaller spacing between the rollers loading (mm).

5. Results and discussion

The identification and characterization procedures aimed to verify whether the characteristics of materials and products are expected in the present work, meet the conditions of sufficient quality when applying the final ceramic as dental materials.

5.1 Characterization of materials

The main objective focuses on the characterization of raw material, identifying the origin of each material used, assessing the crystallographic characteristics and morphological profile

of the post in question. This goal aims to confirm whether such characteristics of powders, and mixtures of the powders were suitable for the final density of sintered.

5.1.1 Microstructural characterization

Powders of Zirconia – $ZrO_2(Y_2O_3)$ – and Bioglass were characterized by SEM and the results are shown in Figures 3 and 4. The zirconia powder used in this study was produced through a spray-drying, with additions of ligands, which promote the agglomeration of spherical shapes, as shown in Figure 3. These ligands are used to facilitate compaction of the samples.

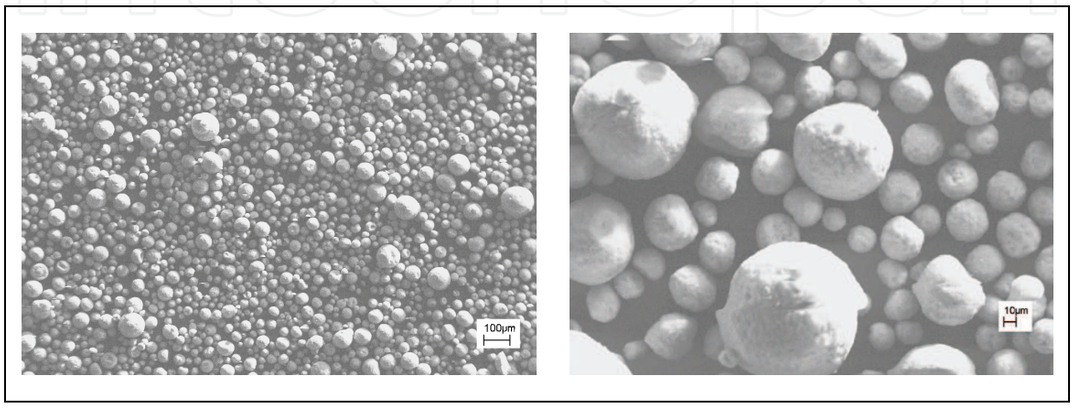

Fig. 3. Particle morphology of $ZrO_2(Y_2O_3)$ as received.

In Figure 4 are performed by SEM micrographs of samples of Bioglass powder, sifted after. One observes the presence of acicular particles presenting larger dimensions than the sieve, the intrinsic characteristics of glassy materials.

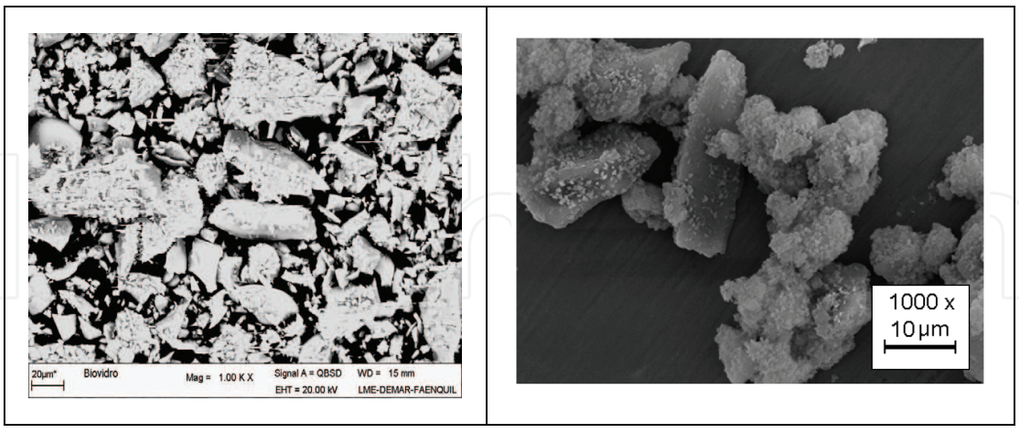

Fig. 4. Morphology of the Bioglass after fragmentation and sieving.

The Bioglasses, after collection, were screened on meshes of up to 32µm in order to minimize the effect of their distribution in the zirconia matrix, increasing the compaction of the mixtures of powders, where the density on the green of the samples ranged from 48% to 42% due to the addition of Bioglass matrix $ZrO_2(Y_2O_3)$. Reducing the particle size of Bioglass facilitating the spreading of the fluid (liquid phase) during the sintering step.

5.1.2 Characterisation of compressed

The green relative density of the compacts are shown in Figure 5.

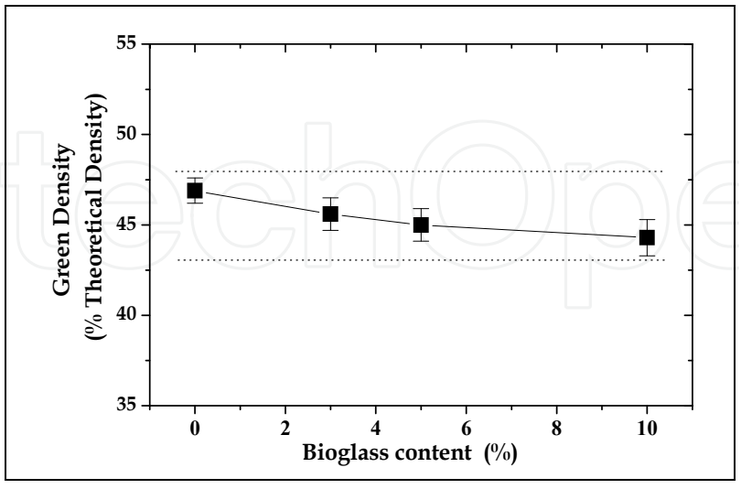

Fig. 5. Effect of the addition of Bioglass on the green density of compacts.

Note that there is a slight reduction in relative density due to the addition of Bioglass in its composition. This behavior occurs through the morphology of Bioglass, highly irregular (Figure 5), compared to the powder of $ZrO_2(Y_3O_2)$, used in these experiments. Be considered negligible differences in green density, sintering behavior observed in the samples with different amounts of Bioglass.

Figure 6 shows representative micrographs of samples sintered at each composition studied. For comparative analysis of dense material, some samples of $ZrO_2(Y_2O_3)$ were without Bioglass sintered at 1500°C/2 hours.

It is observed the presence of equiaxed grains of ZrO_2 in the whole area analyzed. Were obtained in all cases, with 3, 5 or 10wt% of Bioglass, microstructures were quite similar. There is also the presence of voids between grains resulting from the elimination of residual porosity and intergranular phase during thermal attack.

From the micrographs presented in Figure 6 and Table 4.4 lists the microstructural parameters, to verify whether the presence of liquid phase formed from the fusion of glass particles interfered with grain growth of ZrO_2.

Analyzing the results of Table 1 can be stated that the content of Bioglass little or almost nothing, interferes with the average grain size of ZrO_2 and density of grains per unit area, as shown in Figure 6.

These microstructural characteristics are a direct function of initial grain size and sintering temperature used. Dense ZrO_2 sintered solid phase is usually obtained at temperatures around 1500°C. In this temperature range, depending on the sintering time applied, the average grain size can vary from 0.5μm to 1μm, whose sizes are the result of higher levels with very long sintering, such as 1500°C/8h.

The use of relatively low sintering temperatures, as from 1200 to 1350°C, hinders the growth of the grains of the matrix, thus increasing the population of grain per unit area. In this study, the use of liquid phase has as one of several objectives to facilitate the densification at low temperatures, minimizing the grain growth, which could hamper the

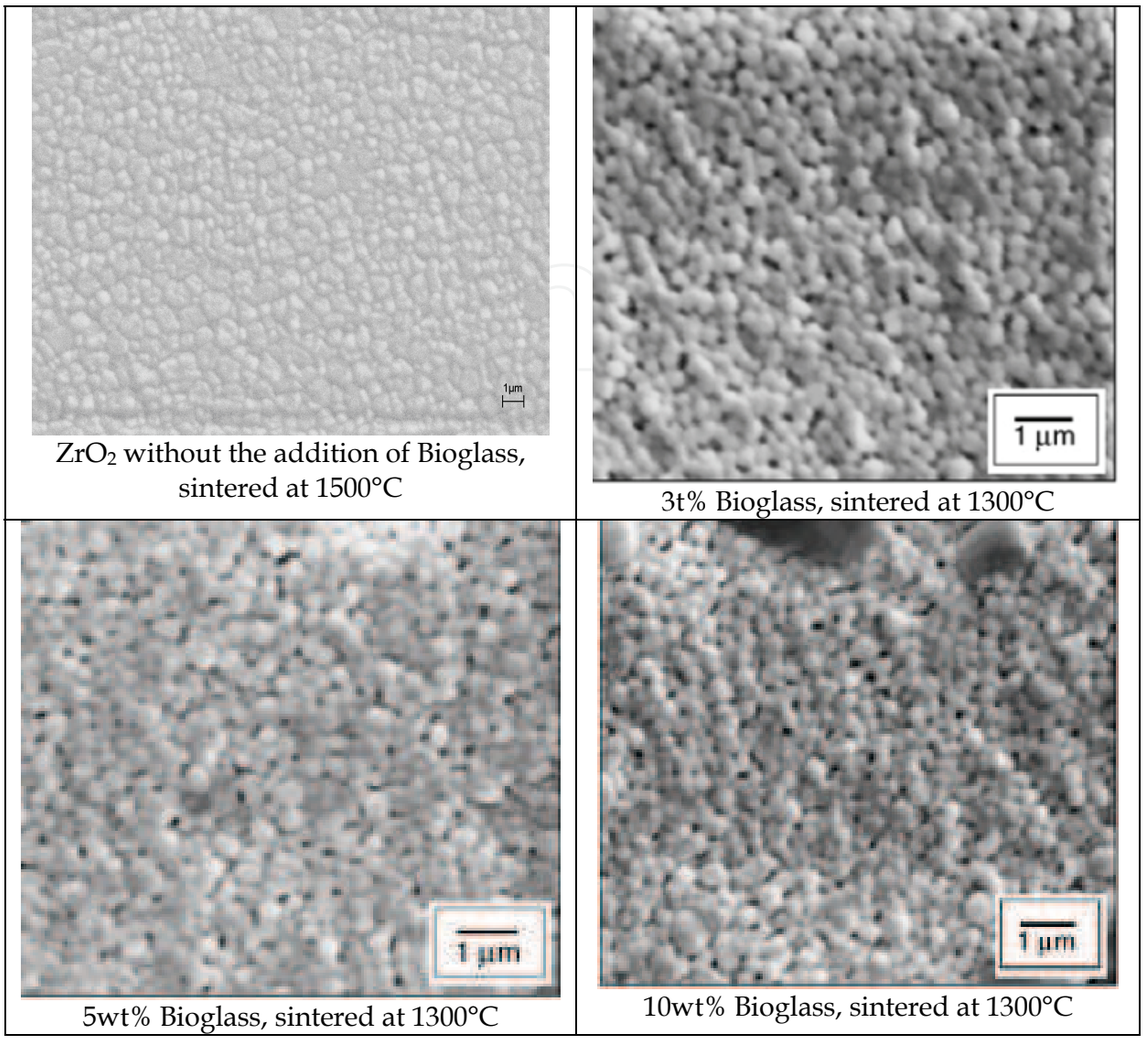

ZrO_2 without the addition of Bioglass, sintered at 1500°C

3t% Bioglass, sintered at 1300°C

5wt% Bioglass, sintered at 1300°C

10wt% Bioglass, sintered at 1300°C

Fig. 6. Micrographs of ceramics $ZrO_2(Y_2O_3)$-Bioglass.

(ZrO_2: Bioglass) wt%	**Medium Size Grain (µm)**	**Density of grains (No. grains /µm²)**
100:00 (1500°C)	0.803 ± 0.121	3.405
97:03	0.325 ± 0.065	9.982
95:05	0.329 ± 0.076	9.964
90:10	0.333 ± 0.070	9.939

Table 1. Parameters microstructure of $ZrO_2(Y_2O_3)$-Bioglass, sintered at 1300°C.

growth and propagation of cracks during the fracture of the material, knowing that the cracks propagate in this material so intergranular (following the grain boundaries), and has also the beneficial effect of martensitic transformation (tetragonal to monoclinic, as indicated by T→M), which occurs when the crack is tetragonal grain, and exerts compressive stress on them.

5.1.3 Dilatometry

These tests are carried out to verify the effect of the addition of Bioglass in the temperature of maximum shrinkage of the sintered body by the derivative of the shrinkage versus time. Thus have been able to verify the relationship between the percentage of Bioglass with the rates of dimensional variation of the material versus time and temperature.

The results of dilatometric analysis performed on samples previously consolidated raw material monolithic, had coefficients of thermal expansion ($\alpha_{200\text{-}1200^oC}$) to $10.6x10^{-6}/^oC$ tetragonal zirconia polycrystal (Y-TZP) and $10.2x10^{-6}/^oC$ for Bioglass.

From the results, there is compatibility between the thermal expansion coefficients of the two phases (ZrO_2-Bioglass) for the formation of the composite ceramic-ceramic primary requirement for development of dual-phase ceramic materials (MEYERS, CHAWLA, 1998), due to reduction of residual stresses are generated between the phases of the composite and rigid after cooling.

Table 2 presents the results of calculations concerning the average values of the coefficients of thermal expansion, carried out for all compositions in this work, based on the weighting between the coefficients of thermal expansion and modulus of elasticity of the components of mixtures. These values are important in determining the residual stress generated between the phases in sintered.

Concentration of Bioglass (wt%)	Bioglass		$ZrO_2(Y_2O_3)$[1]		Composite
	Modulus of Elasticity E (GPa)[2]	Thermal Expansion Coefficient α (x $10^{-6}/^oC$)	Modulus of Elasticity E (GPa)	Thermal Expansion Coefficient α (x $10^{-6}/^oC$)	Thermal Expansion Coefficient α (x $10^{-6}/^oC$)
3					10.599
5	90	10.2	190	10.6	10.594
10					10.587

Table 2. General Physical Characteristics of the composites.

The curves of shrinkage and shrinkage rate as a function of temperature and hold time showed the following highlights:

(i) Part one

Can be analyzed at temperatures up to 600ºC. The most significant variations in this region occur at temperatures around 450°C. At this temperature there is a smooth change of the shrinkage, which can be attributed to the volatilization of organic substances present in the

[1]The results of modulus of elasticity were obtained from the available literature (OLIVEIRA, 1997)
[2]Manufacturer's data.

compact. These are derived from organic raw material, $ZrO_2(Y_2O_3)$, which has a binder, and stearin used in compaction of powders.

(ii) Part two

The region represents the effect of temperature on the shrinkage of compacts, observed from 1,050°C. Observe that there is a characteristic temperature where the rate of shrinkage has a maximum.

Figure 7 shows the temperatures of shrinkage depending on the content of Bioglass. In this figure are also presented as the accumulated instantaneous values of shrinkage at these temperatures.

It is observed that the samples are reduced maximum temperature decrease with increasing amount of Bioglass added. This behavior implies that a larger amount of glass reduces the temperature, the greater formation of liquid phase, which in turn allows a greater shrinkage of the compact. Samples without the presence of additives, have different behavior, because it is sintered by solid phase, and therefore governed by other mechanisms of sintering.

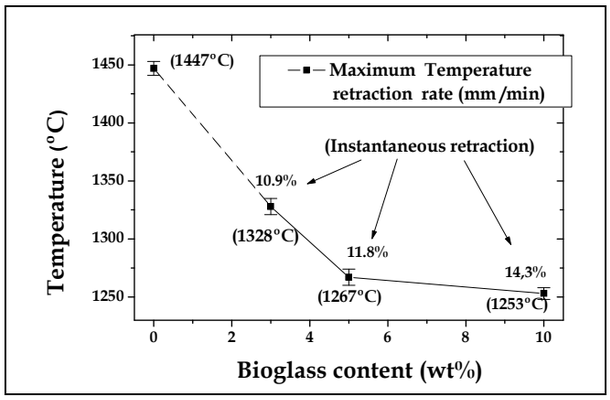

Fig. 7. Effect of the addition of Bioglass in the temperatures of greatest rate of shrinkage.

It was observed that for samples with 3wt% of Bioglass, at temperatures below 1300°C, was not reached maximum retraction of the derivative and thus, levels of incorporation of the sintering cycle time initially proposed.

The temperatures of maximum shrinkage determined for samples with 5 and 10wt% of Bioglass are respectively 1267°C and 1253°C.

(iii) Third party

In this third area of analysis is taken into account the hold time at 1300°C. From the analysis of Figure7, we observed that the samples with higher concentrations of Bioglass, achieved larger decreases until the maximum temperature testing (1300 ° C).

From there, observing Figure 8, note that there is an evolution of the shrinkage in the first minutes of landing, in all situations where Bioglass is used as an additive. Comparatively, the blocks of ZrO_2 sintered without the addition of Bioglass show continued growth as a function of hold time, because the weather influences the kinetics of densification of the sintered solid phase.

Observe that the first 20 minutes, in samples with Bioglass, retractions that occur faster when compared with the remaining time, always with a tendency to stabilize the rate of shrinkage (indicated by the rate of change of the curve). Both the rate of shrinkage and total

shrinkage increases with increasing content of Bioglass. This is justified by the greater amount of liquid phase which facilitates the diffusion of the solid phase.

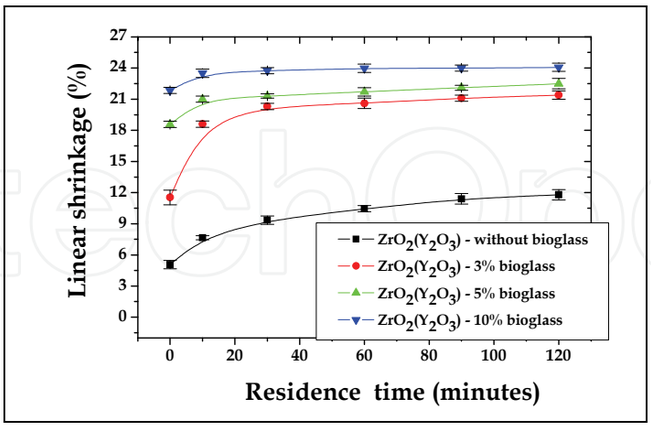

Fig. 8. Effect of isotherm plateau in shrinkage of the ceramics sintered at 1,300ºC.

The results seen above can be represented in percentage gains of shrinkage versus time of isotherm used. These results are shown in Figures 9 and 10.
An important detail presented by the geometrical behavior of the curves with respect to the correlation between the percentage increase in Bioglass and gain decrease with residence time at 1300°C. The three curves show asymptotic behavior, with the rate of linear shrinkage with time tends to proportionality with the difference between the instantaneous rate and a maximum rate for each composition in Bioglass. Larger amounts of Bioglass cause lower coefficients of thermal expansion, in agreement with Table 2. Add to it that lower the green density implies an increase of spaces to be filled, so it will have a higher rate of shrinkage.

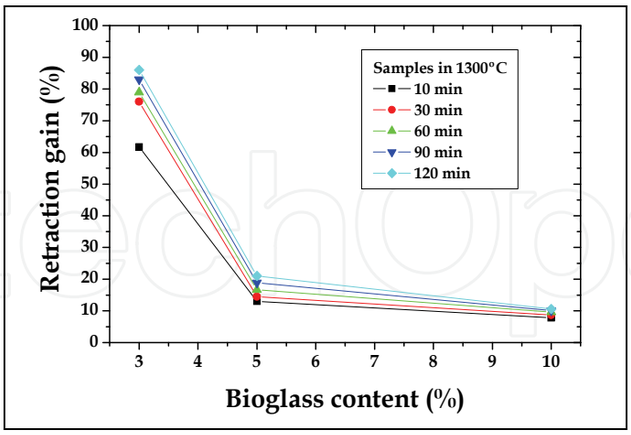

Fig. 9. Gains due to shrinkage of the content of Bioglass, for various treatment times.

It is evident that the ceramics with 3wt% of Bioglass have improved significantly with the use of level of sintering. At first, with 10 minutes of landing, there is a gain of 60%, indicating that this time was sufficient to reduce the viscosity of the glass, influencing their spread around the ZrO_2 grains. Times lead to higher cumulative gains exceeding 85%, as in 120 minutes. Samples with 5 and 10wt% are less influenced by the time of landing, for

sintering at 1300ºC. Still, for the maximum times studied, 120 minutes, occur up to 20% gains, for ceramics with 5wt% Bioglass and 10% for ceramics with 10wt% of Bioglass. The level of decline observed in the samples will indicate that in all situations where Bioglass was used as an additive, and 1300°C, there is full densification of the ceramics studied. In the case of the ceramics of $ZrO_2(Y_2O_3)$, without addition of glass-forming liquid phase, the phenomenon does not occur.

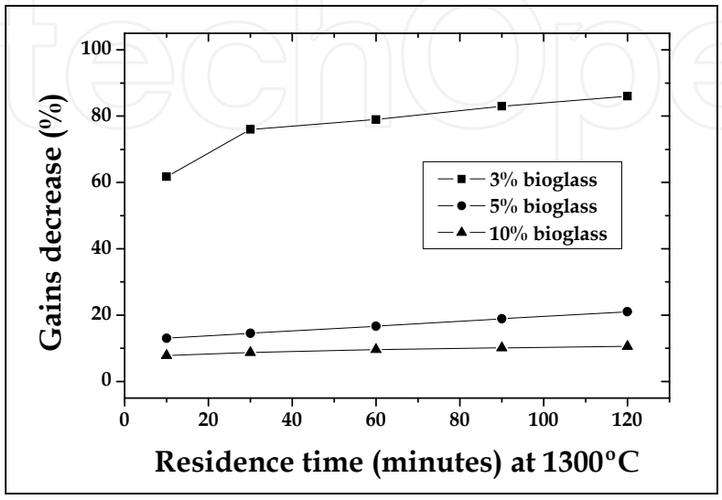

Fig. 10. Gains decrease as a function of residence time, for each composition of Bioglass.

5.2 Characterization of the sintered samples

It is intended to report the results of analysis of the crystalline phases present in sintered samples, and studies the influence of Bioglass content on densification. With this it will have the assurance that the sintering conditions (temperature, time, rate of heating and cooling) were adequate for obtaining ceramics with adequate strength for use in dental applications.
The research initiated by Habibe (HABIBE, 2007) showed that the addition of Bioglass in higher sintered $ZrO_2(Y_2O_3)$ to provide undesirable martensitic transformation (T→M), which promote a volumetric expansion of the ceramic matrix generating increasing porosity. One concern has been established to optimize the densification, taking into account the interrelationship between low sintering temperature, sintering time and microstructural features.

5.2.1 Crystallographic characterization

In order to demonstrate the efficiency of the technique of X-Ray Diffraction in the characterization and measurement of the percentage of monoclinic and tetragonal phases of $ZrO_2(Y_2O_3)$ was proposed in this study, the use of determining the depth of penetration of radiation, based on parameters crystallographic theory.
Using the parameters presented the results obtained when applying these equations (3 and 4), was approximately 7.3μm. Grain sizes are below 0.5μm, so there is a layer thick enough to be detected by diffraction, thus allowing the identification of transformation of monoclinic phase in sub-surface levels with considerable degree of accuracy.
In pre-existing glasses of similar chemical composition to this study, obtained under the same conditions of melting and cooling, gave values of Vickers hardness near 6.2GPa, when

subjected to thermal treatment time exceeding 30 minutes. The values of fracture toughness and resistance to bending found were 0.93MPa.m$^{1/2}$ and 54MPa, respectively, for materials with rapid cooling (diamonds), and the values of 1.4MPa.m$^{1/2}$ and 115MPa, respectively, for materials with slow cooling (vitro-ceramic) (OLIVEIRA, 1997).
The percentage of transformed monoclinic phase after sintering, carried out according to Equations 1 and 2 are presented in Table 3 and illustrated in Figure 11.

Bioglass wt%	Monoclinic %
0	5.69 ± 0.02
3	6.71 ± 0.06
5	8.75 ± 0.03
10	14.37 ± 0.05

Table 3. Percentage of monoclinic phase in the sintered samples.

This behavior may be related to the gradient of contraction between the two phases (zirconia and Bioglass) after sintering, during cooling, since there is a difference between the thermal expansion coefficients between these materials (10.6x10^{-6}/°C for zirconia and the Bioglass 10.2x10^{-6}/°C). This difference promotes the generation of stress fields around the grains of $ZrO_2(Y_2O_3)$, which may exceed the maximum compressive stress needed to transform the tetragonal-monoclinic. Thus, the grains of $ZrO_2(Y_2O_3)$ tetragonal become monoclinic, with volume expansion of about 3 to 6% by volume (STEVENS, 1986), resulting in an overall structure microcracking, resulting in a reduction in density on the sample. In Figure 4.24 are the results related to this characterization.

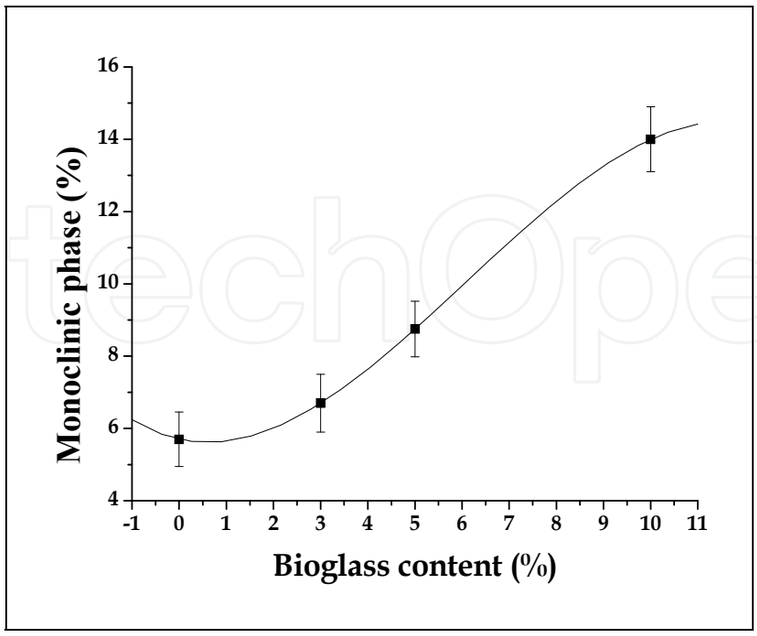

Fig. 11. Monoclinic phase concentration depending on the content of Bioglass in blocks sintered at 1300ºC.

5.2.2 Relative density

As previously noted, there is elevation of monoclinic fraction considering increasing the amount of additive. Associated with this transformation occurred during cooling, which is due to thermal residual stress motivated by the difference in thermal expansion coefficient between the phases, may be the reason for the reduction of relative density versus the contents of Bioglass as shown in Figure 12.

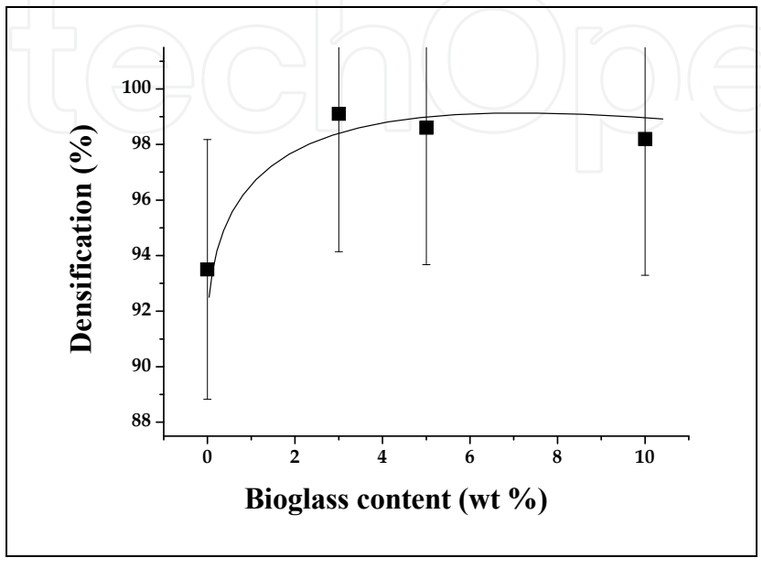

Fig. 12. Relative density as a function of the content of Bioglass, sintered blocks to 1,300°C.

The analysis of X-ray diffraction patterns indicated the presence of considerable fraction of the tetragonal phase and residual fraction of monoclinic phase. Intergranular crystalline phases were not detected in any of sintered body, indicating that the intergranular phase of Bioglass originally made can be fully amorphous or so, the fractions present in the sintered samples are not detected in the diffractometer. This can be considered in the light of that, in previous work (OLIVEIRA et al., 1997).

Bioglass cold considering controlled rates similar to those used in this study (10°C/min) showed the crystalline phases whitlockite and enstatite, and this last was not observed in this work. The possible crystallization of the Bioglass used in this work, and therefore the glass ceramics, may have contributed to the improvement of mechanical properties, with the increase in resistance (60 to 120MPa) and fracture toughness (1 to 1.5MPa.$m^{1/2}$) in the glassy phase (OLIVEIRA et al., 1997).

It is noteworthy that the material exhibits a tendency to decrease the densification with increasing amounts of Bioglass from 3wt%, and these results imply a direct function of increasing content of monoclinic phase transformed. Furthermore, the low density results on the composition submitted for "100-00", suitable only for comparison purposes, since this is accomplished by sintering the solid phase, since there have Bioglass in its composition, which could trigger mechanisms unique liquid phase sintering.

The results indicated that the dilatometry samples monolithic $ZrO_2(Y_2O_3)$ did not densify under these conditions because temperature and isothermal sintering times studied did not allow the efficient operation of the mechanisms for densification of the material. Moreover, samples with Bioglass showed maximum shrinkage temperature of about 1253, 1267 and

1328°C, for contents of Bioglass 10, 5 and 3wt% respectively. In all cases where it is applied Bioglass need for isothermal sintering at 1300°C for full densification is achieved. However, higher levels of Bioglass ($ZrO_2(Y_2O_3)$ containing 10wt% Bioglass) did not allow full densification, because during cooling, as proposed by previous study Habibe (HABIBE, 2007), there is generation of stress fields between the matrix and grain boundaries which promotes the phase transformation (T→M) that generates volume expansion and increased presence of pores and microcracks.

5.2.3 Critical failure size vs. surface roughness

The flexural strength, σ_f, the ceramic is directly proportional to the fracture toughness, K_{IC}, as predicted by linear elastic fracture mechanics (KIM et al., 2000):

$$\sigma = \frac{K_{IC}}{\sqrt{\pi c}} \tag{6}$$

The parameter "c" can be considered alternatively as the size of failure to initiate the fracture. Thus, the size of failure for start of fracture in samples of 3, 5 or 10wt% of Bioglass and sintered at 1300°C/2h, are valued between 80μm and 230μm.

The maximum surface roughness, assessed during the preparation of specimens for bending tests/fatigue, was less than 0.30μm. Whereas the roughness implies that a 'valley' is half of a crack, it is concluded that the roughness used did not affect the test results.

5.3 Mechanical properties

5.3.1 Vickers hardness and fracture toughness

Table 4 and Figure 13 present the results of Vickers hardness and fracture toughness, K_{IC}, the samples sintered at different temperatures and fractional percentages of Bioglass.

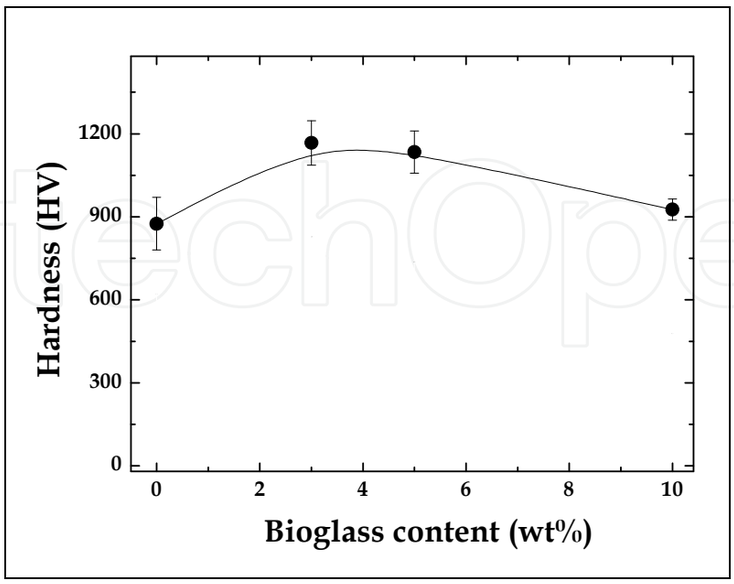

Fig. 13. Hardness of sintered samples as a function of sintering temperature and amount of Bioglass.

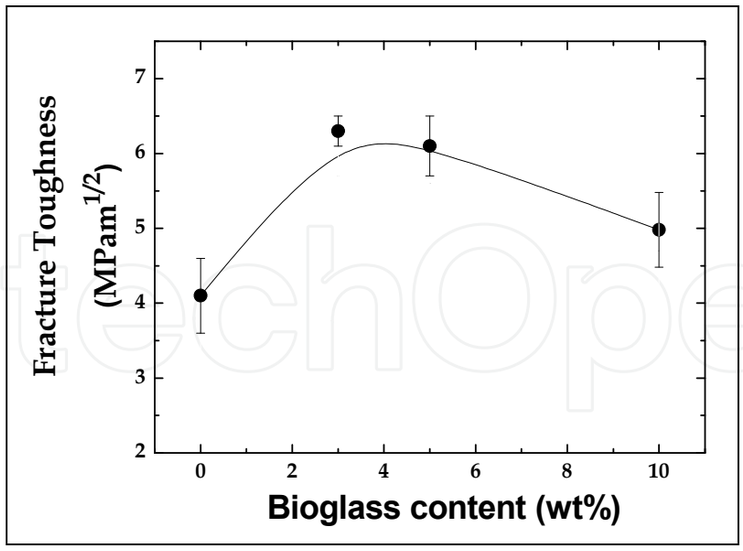

Fig. 14. Fracture toughness of sintered samples as a function of sintering temperature and amount of Bioglass.

The samples sintered at 1300ºC, containing 3wt% of Bioglass showed higher hardness and toughness, respectively, 1170HV and 6.3MPa.m$^{1/2}$. These results are related to indicators of relative density and low amount of martensitic transformation, shown in Figures 14 and 15. It is important to note that these samples show the best properties, possibly due to the high relative density, coming from the better spreading of the liquid formed during sintering and its penetration around the ZrO_2 particles. These phenomenons facilitates the elimination of pores and reduce accumulation of glass triple joints, minimizing the generation of stress fields during cooling and therefore points in favor of crack propagation.

5.3.2 Flexural strength

Samples of $ZrO_2(Y_2O_3)$, with addition of Bioglass, sintered at 1300ºC and without addition of Bioglass (sintered at 1500ºC) were tested for 4 point bending. The results are presented in Table 4 in Figure15.

Bioglass (wt %)	Vickers Hardness (HV)	K_{IC} (MPa.m$^{1/2}$)	Flexural Strength (MPa)
0 (1500ºC)	875 ± 95	4.1 ± 0.5	127.44 ± 57.15
3	1,167 ± 80	6.3 ± 0.2	453.28 ± 74.64
5	1,134 ± 76	6.1 ± 0.4	363.31 ±54.88
10	926 ± 38	5.0 ± 0.5	303.00 ± 77.40

Table 4. Vickers hardness, fracture toughness and Flexural strength of samples sintered.

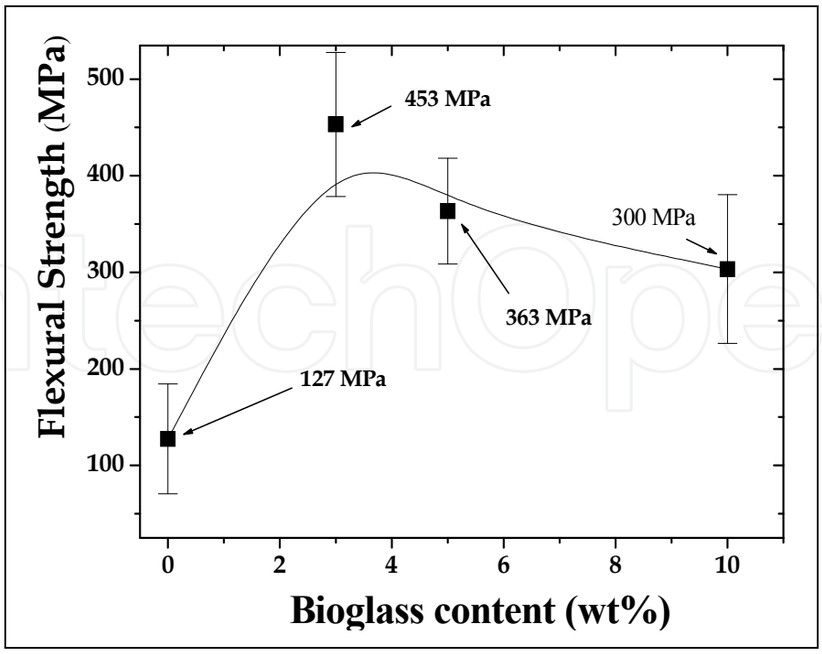

Fig. 15. Flexural strength of samples sintered at 1300°C, depending on the amount of Bioglass added to ZrO_2 matrix.

It is observed that the variations in the composition in the flexural strength is shown similar to those observed in the behavior of relative density (Figure 12), hardness (Figure 13) and fracture toughness (Figure 14), ie, an elevation in the range from zero to 3wt% Bioglass and reduction in the range of 3 to 5wt% Bioglass. Such behavior suggests that the 3wt% level gives better distribution in the zirconia matrix, leading to the conclusion that the higher values are dispersed causing islands to concentrate on Bioglass, causing some weakening and partial degradation of those characteristics. Such behavior is indicative of the concentration 3wt% Bioglass in $ZrO_2(Y_2O_3)$ would be the best choice among the four discussed compositions. This without taking into account other factors that could influence the choice.

5.3.3 Residual stresses

The calculation of the average thermal residual stress generated during cooling of the sintered samples was based on the consideration that there is homogeneous distribution of second phase in ceramic matrix ZrO_2, and is directly related to the difference in thermal expansion coefficients between the phases in the ZrO_2 matrix and intergranular glassy phase, composed of Bioglass (TAYA et al., 1990; SHI et al., 1998).

Was not taken into account the hypothesis of partial crystallization of the glass or the temperature range where there is softening of the glass present. This average residual thermal stress in the two phases can be calculated as a function of the percentage of intergranular phase (or second) that integrates the system, according to Equations 7 and 8, proposed by Shi (SHI et al., 2000).

$$\sigma_b = E_b\left(\langle\alpha\rangle - \alpha_b\right)\Delta T \tag{7}$$

$$\sigma_m = E_m\left(\langle\alpha\rangle - \alpha_m\right)\Delta T \tag{8}$$

Where σ_b and σ_m are the contours and residual stresses in the matrix, respectively. E_m and E_b indicate the modulus of elasticity of matrix and grain boundaries (intergranular phase), respectively, and α, α_m and α_b indicate the average thermal expansion coefficients, the matrix (index m) and the intergranular phase (index b), respectively. The average coefficient of thermal expansion of each composition varies, and is given by Equation 9:

$$\langle\alpha\rangle = \frac{\alpha_b C_b E_b + \alpha_m C_m E_m}{C_b E_b + C_m E_m} \tag{9}$$

Where $\langle\alpha\rangle$ is the coefficient of thermal expansion of the composition; α_b, C_b, E_b are, respectively, coefficient of thermal expansion, Young's modulus and fraction of Bioglass (grain boundary), α_m, C_m, E_m are respectively, the coefficient of thermal expansion, the fraction and the modulus of elasticity of ZrO_2 matrix.

By calculating the average coefficient of thermal expansion and residual stresses, it is found that when $\alpha_m > \alpha_b$ or $\sigma_b < 0$, the grain boundary is the transition between compression (intragranular) and tensile (matrix).

The residual stress in a multiphase composite is developed due to the discrepancy between the modulus of elasticity and Thermal Expansion Coefficient (TEC) between the constituent phases. Due to the lower TEC of Bioglass, α_b, compared to the array of ZrO_2, α_m, tensile residual stresses are developed in ZrO_2 matrix during cooling from the sintering temperature. (BASU, VLEUGELS, 2001).

The residual stress in zirconia matrix was calculated according to the model proposed by Taya (TAYA et al., 1990) and confirmed by Shi (SHI et al., 2000). In the calculations we used the modulus of elasticity (E) from 90GPa to 190GPa for the Bioglass and ZrO_2. The calculation results of compressive residual stress at grain boundaries and tensile stress in the grains of ZrO_2 matrix are shown in Figure 16, and provide a barrier to crack propagation, toughened materials.

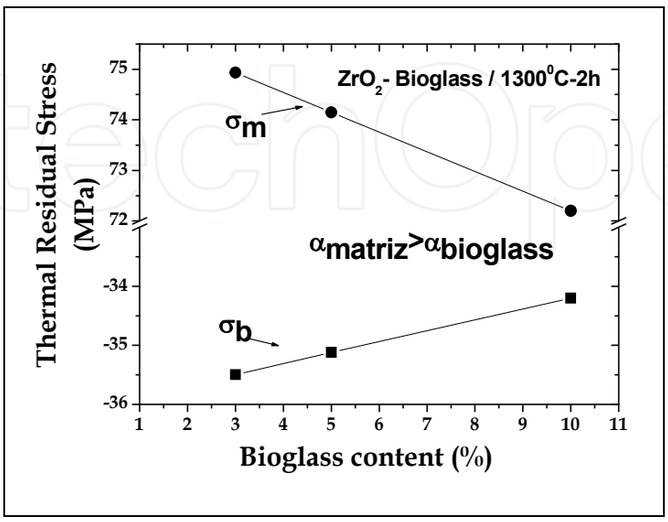

Fig. 16. Thermal residual stress due to the content of Bioglass (intergranular phase)

The toughening of ceramics developed in this work may be related to several phenomena, such as tetragonal-monoclinic transformation, crack deflection, stress-induced martensitic transformation thermal residual porosity of the sintered samples, or other possible causes unrelated. It may be noted that increasing the intergranular phase (Bioglass) leads to increased % of monoclinic phase and increased porosity associated with this phenomenon.
However, increasing the amount of Bioglass leads to a greater accumulation of concentrations of glass in triple junctions, with consequent formation of stress concentration, which permits growth and propagation of cracks. The thermal residual stresses in ZrO_2 matrix show a smaller and smaller effect as a function of the addition of Bioglass composition. However, there is a reduction in the contribution of residual stress on phase transformation (T→M), which can improve the toughness of ceramics.
Moreover, the presence of low amounts of Bioglass, facilitates the diffusional processes, reduce the possibility of transformation (T→M) to occur during cooling and increase the thermal residual stress between the phases, favoring the phase transformation during the emergence and growth of a crack, toughened material.
Previous studies have shown that propagation of intergranular cracks of the type prevalent in ZrO_2 based ceramic sintered by liquid phase (SHI et al., 1998, SUN et al., 2003, HUANG et al., 2003, SHI et al., 2000) due to the presence of glassy phase. The amount of intergranular phase in which the fracture toughness (K_{IC}), the maximum can be achieved, $C_{b,m}$, when $\alpha_b < \sigma_m$, is as follows:

$$C_{b,m} = \frac{\alpha_m - \alpha_b}{3\left(\alpha_m - \frac{E_b}{E_m}\alpha_b\right)} \tag{10}$$

Where α_b E_b are the Thermal Expansion Coefficient (TEC) and Modulus of Elasticity of Bioglass, respectively, and α_m, and E_m are, respectively, the Thermal Expansion Coefficient and Modulus of Elasticity of ZrO_2 matrix.
The calculated results show that a great theoretical value is achieved with 2.84wt% of Bioglass. This result is consistent with the composition of ZrO_2-Bioglass composite composed of 97wt% ZrO_2 and 3wt% Bioglass, which presents the best mechanical properties among the samples sintered at 1300°C/2h. Moreover, the results are consistent with previous work (SHI et al., 2000), which shows that only a small amount of intergranular glassy phase, an increase of fracture toughness can be obtained.

6. Conclusions

After the experiments, and based on these results, we can conclude that:

1. Samples of 3wt% Bioglass composition showed better densification compared to those of composition 0, 5 and 10wt% due to better spreading of the liquid phase between grains of $ZrO_2(Y_2O_3)$. These results are related to high density and low percentage of monoclinic ZrO_2 phase, present in the sintered samples.
2. The addition of higher concentrations of additives in an increase in 'islands' of Bioglass, the junctions between the grains of the matrix of $ZrO_2(Y_2O_3)$ causing residual stress fields, which led to greater amounts of martensitic transformations, after sintering, increasing the weakening of the material.

3. The results of mechanical characterization promote the use of Bioglass as sintering additive, instead of $ZrO_2(Y_2O_3)$ pure. Using the techniques of X-Ray Diffraction, high resolution, together with testing the hardness, fracture toughness, flexural strength at 4 points confirmed this statement.
4. The ceramic compositions suggested for studies, combined with the processing conditions (parameters of milling, pressing and sintering) were effective in obtaining the ceramic bodies of high relative density and with relatively fine grain. Regardless of the content of Bioglass added to zirconia, the average grain size of zirconia was in the order 0.30 to 0.35 μm.
5. The additions of 3 and 5% of Bioglass produced an increase in hardness in relation to zirconia with 3wt%Y_2O_3, and also in relation to the addition of 10wt% of Bioglass, with values of 1240 and 1210HV for 3Y-TZP composites-Bioglass (97-3) and 3Y-TZP-Bioglass (95-5), respectively. These results are due to higher densification of samples submitted for 3wt% of Bioglass.

7. Acknowledgment

The authors acknowledge to the FAPESP for financial support, under Grants no. 04/04386-1 and 05/52971-3. They also thank the Fundação Euclides da Cunha - Universidade Federal Fluminense.

8. References

Amaral, M.; Lopes, M.A.; Silva, R.F.; Santos, J.D. (2002). Densification route of Si_3N_4 – Bioglass biocomposites. *Biomaterials,* v.23, p.857-862.

Anusavice, K. J. (2005); *Phillips Materiais Dentários*. 11a Ed. Rio de Janeiro; Elsevier Editora. ISBN: 9788535215328.

Basu, D., Sarkar, B. K. Effect of zirconia addition on the fatigue behaviour of fine grained alumina. Bull. *Materials Science Forum*, v. 24, n. 2, p.101-104, Apr, 201. ISSN: 0255-5476

Bicalho, L. A.; Souza, R.C.; Santos; C.; Barboza, M. J. R.; Baptista, C.A.R.P. (2008). Fatigue of Zirconia - Bioglass Dental Ceramics. *Materials Science Forum,* v. 591-593, p.628-633. ISSN: 0255-5476

Bicalho, L. A.; Santos, C.; Souza, R. C.; Barboza, M. J. R.; Baptista, C.A.R.P. (2010). Mechanical behavior of ZrO_2-Bioglass dental ceramics under cyclic fatigue loading. *Materials Science Forum*, v. 636-37, p. 47-53. ISSN: 0255-5476

Bicalho , L. A. ; Santos, C. ; Habibe, A. F. ; Souza, R. C. ; Barboza, M. J. R. ; Baptista, C. A. R. P. (2007) Performance of ZrO_2-Bioglass Dental Ceramics under Cyclic Fatigue Loading. *Cadernos UniFOA*, v. 2, p. 30-33.

Bicalho, L. A.; Santos, C.; Barboza, M. J. R.; Moreira, M. E. S.; Strecker, K. (2010) . Investigation of the sinterability of $ZrO_2(Y_2O_3)$-Bioglass dental ceramics by dilatometry. In: *The 6th Latin American Congress of Artificial Organs and Biomaterials*, august-2010. Gramado-RS, Brazil. Proceedings of the 6th COLAOB, v. 1. p. 1-8.

Habibe, A. F. (2007). Desenvolvimento e caracterização de cerâmicas à base de ZrO_2 utilizando um biovidro do sistema $3CaO.P_2O_5$-SiO_2-MgO como aditivo de sinterização. 123f.; *MsC Dissertation in Materials Science.* Escola de Engenharia de Lorena - Universidade de São Paulo, Lorena, Brasil.

Huang, X.W.; Wang, S. W.; Huang, X. X. (2003). Micoestruture and mechanical properties of ZTA fabricated by liquid phase sintering. *Ceramics International*, v.29, p.765-769, 2003. ISSN: 0272-8842.

Huang, X.W.; Wang, S. W.; Huang, X. X. (2003). Micoestruture and mechanical properties of ZTA fabricated by liquid phase sintering. *Ceramics International,* v.29, p.765-769. ISSN: 0272-8842.

JCPDS – Powder Diffraction File Search Manual. Hanawalt Method Inorganic. (1998), USA. *Published by the International Center for Diffraction Data.*

Kelly, J. R.(1997). Ceramics in restorative and prosthetic dentistry. *Annuary of review in Material Science.*, v.27, p. 443–68, 1997.

Kim, D.-J., Lee, M.-H., Lee, D. Y., Han, J.-S. (2000). Mechanical Properties, Phase Stability, and Biocompatibility of (Y,Nb)-TZP/Al_2O_3 Composite Abutments for Dental Implant. *Journal of Biomedical Material Research,* v.53, n.4, p. 438-443. ISSN (printed): 1549-3296.

Klug, H. P.; Alexander, L. E. (1974). X-Ray Diffraction Procedures for Polycristllines and Amorphous materials. *John Wley and Sons*, New York.

kohn D. H.; Ducheyne P.; Awerbuch, J. (1992). Acoustic emission during fatigue of porous-coated Ti-6Al-4V implant alloy. *Journal of Biomedical Materials Research*, v. 26, n.1, p.19-38 January 1992. ISSN (printed): 1549-3296,

Kohn, D. H., Ducheyne P., Awerbuch, J. (1992). Sources of acoustic emission during fatigue of Ti-6Al-4V: effect of microstructure: *Journal of Materials Science*. v.27, n. 6, p.1633–1641. ISSN: 0022-2461,

Maeda, L. D. ; Habibe, A. F. ; Santos, C. ; Daguano, J. K. M. F. ; Bicalho, L. A. ; Souza, R. C. ; Barboza, M. J. R. (2007). Efeito da adição de Biovidro na resistência à fratura dos compósitos biocerâmicos ZrO_2-biovidro. In: 51º Congresso Brasileiro de Cerâmica, Salvador-BA, Brazil. Proceedings of 51º CBC-Congresso Brasileiro de Cerâmica, v. 1.

Meyers, M. A., Chawla, K. K. (1982). Princípios de Metalurgia Mecânica. Edgard Blücher. São Paulo.

Oliveira, A. P. A. (1997). Influência de fatores físico-químicos na produção de pós de zircônia. *Doctoral Thesis* . PUC-RJ.

Oliveira, J. M.; Fernandes, M. H.; Correia, R. N. (1997). Development of a New Glass Ceramic in the System MgO-3CaO.P_2O_5-SiO_2. *Bioceramics,* v.5, p. 7-14. ISSN (electronic): 2090-5025.

Santos, C.; Souza, R. C. ; Barboza, M. J. R. ; Bicalho, L. A. ; Baptista, C.A.R.P. ; Strecker, K. (2009). Fatigue Behavior of dental ceramics based on Zr_2O-Al_2O_3 composites. In: *64º Congresso anual da ABM*, Belo Horizonte. Anais do 64º Congresso ABM, lulho-2009. v. 1. p. 1-10.

Shi, J. L., Lu, Z. L., Guo, J. K. (2000). Model analysis of boundary residual stress and its effect on toughness in thin boundary layered yttria-stabilized tetragonal zirconia polycrystalline ceramics. *Journal of Materials Research,* v.15, n.3, p.727-732.

Shi, J. L.; Li, L. Guo, J .K. (1998). Boundary stress and its effect on toughness in thin boundary layered and particulate composites: model analysis and experimental test on T-TZP based ceramic composites. *Journal of the European Ceramic Society*, v.18, p.2035-2043, 1998.

Stevens, R. (1986). An introduction to zirconia: zirconia and zirconia ceramics. [S.L.]. 2nd Ed *Twickenham: Magnesium elektron*.

Sun, Y.-H. Zhanga, Y-F. Guo, J-K. (2003). Microstructure and bending strength of 3Y-TZP ceramics by liquid-phase sintering with CAS addition. *Ceramics International*. v.29, p.229-232. ISSN: 0272-8842.

Taya, M.; et al. (1990). Toughening of a particulate-reinforced ceramic-matrix composite by thermal residual stress. *Journal of the American Ceramic Society*, v.73, n.5, p.1382-1391.

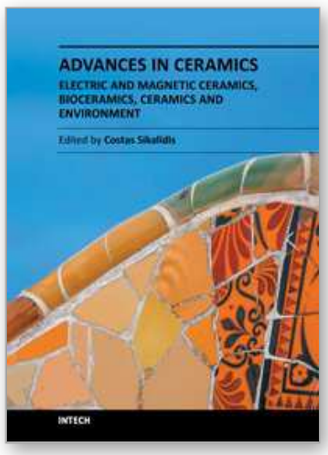

Advances in Ceramics - Electric and Magnetic Ceramics, Bioceramics, Ceramics and Environment

Edited by Prof. Costas Sikalidis

ISBN 978-953-307-350-7
Hard cover, 550 pages
Publisher InTech
Published online 06, September, 2011
Published in print edition September, 2011

The current book consists of twenty-four chapters divided into three sections. Section I includes fourteen chapters in electric and magnetic ceramics which deal with modern specific research on dielectrics and their applications, on nanodielectrics, on piezoceramics, on glass ceramics with para-, anti- or ferro-electric active phases, of varistors ceramics and magnetic ceramics. Section II includes seven chapters in bioceramics which include review information and research results/data on biocompatibility, on medical applications of alumina, zirconia, silicon nitride, ZrO2, bioglass, apatite-wollastonite glass ceramic and b-tri-calcium phosphate. Section III includes three chapters in applications of ceramics in environmental improvement and protection, in water cleaning, in metal bearing wastes stabilization and in utilization of wastes from ceramic industry in concrete and concrete products.

INTECH
open science | open minds

InTech Europe
University Campus STeP Ri
Slavka Krautzeka 83/A
51000 Rijeka, Croatia
Phone: +385 (51) 770 447
Fax: +385 (51) 686 166
www.intechopen.com

InTech China
Unit 405, Office Block, Hotel Equatorial Shanghai
No.65, Yan An Road (West), Shanghai, 200040, China
中国上海市延安西路65号上海国际贵都大饭店办公楼405单元
Phone: +86-21-62489820
Fax: +86-21-62489821

IntechOpen